Hyperfine Interactions 30(1986)337 – 353

DETERMINATION OF FINE AND HYPERFINE STRUCTURE IN Fe-Mo(W) DINUCLEAR CLUSTERS

V. PAPAEFTHYMIOU*, A. SIMOPOULOS, A. KOSTIKAS

Nuclear Research Center Demokritos, 15 310, Aghia Paraskevi, Attiki, Greece

and

D. COUCOUVANIS

Chemistry Department, University of Michigan, Ann Arbor, Michigan 48109, USA

Received 29 April 1986

The fine and hyperfine structure of two dinuclear sulfide bridged Fe-Mo complex anions and their W homologues have been studied by magnetic susceptibility and Mössbauer measurements. It is shown that, by following a stepwise methodology, it is possible to derive from the low temperature magnetization data the value and sign of the fine structure parameters D and E/D. These parameters are further confirmed by an independent analysis of the Mössbauer data. Magnetic and electric hyperfine interaction parameters are also determined from the Mössbauer results. Both fine and hyperfine parameters point to a valence scheme, for all complexes, of Fe^{II}-$Mo^{VI}(W^{VI})$ with a varying degree of charge delocalization from the iron to the molybdenum (tungsten) site. The parameter D is negative with an orientation of its z axis close to the V_{zz} axis.

1. Introduction

A number of heterometallic Fe-Mo-S complexes have been synthesized in recent years in an effort to simulate the active site of the nitrogen fixing enzyme nitrogenase [1]. Among others, we have performed a detailed study of the following four dinuclear complexes:

A : $[(C_6H_5)_4P]_2$ $[(C_2H_5S)_2\ FeS_2MoS_2]$
A* : $[(C_6H_5)_4P]_2$ $[(C_2H_5S)_2\ FeS_2WS_2]$
B : $[(C_6H_5)_4P]_2$ $[(S_5)FeS_2MoS_2]$
B* : $[(C_6H_5)_4P]_2$ $[(S_5)FeS_2WS_2]$.

---

*Present address: Gray Freshwater Biological Institute, University of Minnesota, P.O. Box 100, Navarre, MN 55392, USA.

Details on syntheses, crystal and molecular structure and basic characteristics of the ground-state electronic structure have been published recently [2]. The latter has been determined by an analysis of the magnetic susceptibility and Mössbauer measurements of these samples. The determination of the fine and hyperfine parameters in such complex systems usually presents difficulties which are primarily due to the large number of the unknown parameters.

We present in this paper a detailed analysis of these measurements. It is shown that, by following a certain methodology in relation to general calculations of the magnetic properties of the ^5D state of the iron ion, it is possible to determine with satisfactory confidence the parameters of the fine structure of the complexes from the magnetic susceptibility measurements. A similar approach is followed for an independent determination of these parameters from the Mössbauer spectra. Finally, these parameters are used to extract information related to relaxation rates of the electronic spin system by computation of Mössbauer line shapes.

2. Experimental methods

Magnetic susceptibilities were measured by using a PAR vibrating sample magnetometer equipped with a variable temperature cryostat operating in the range 1.5–300 K and an electromagnet for magnetic fields up to 2 T. Particular care was taken for corrections arising from the holder contribution. This contribution was determined as a function of temperature and magnetic field by measuring the holder filled with a known diamagnetic material. (We have noticed that measurements of empty holders may lead to erroneous results due to the varying amount of paramagnetic oxygen contained in the holders.)

Mössbauer measurements were performed with a constant acceleration spectrometer using a ^{57}Co(Rh) source kept at room temperature. Spectra were collected in the temperature range 1.1–300 K and in external magnetic fields up to 6.0 T applied perpendicular to the direction of γ-rays.

3. Analytical methods

In all cases, the Fe ions are located at the center of distorted sulfur tetrahedra. The structures of the dinuclear complexes are described in terms of the edge-sharing MS_4 (M = Mo, W) and L_2FeS_2 tetrahedral units (L = PhS^- or L_2 = S_5^{2-}) [2]. The effective magnetic moment for all samples is 4.9 Bohr magnetons per formula unit, corresponding to an $S = 2$ spin state for the electronic ground state of the cluster. Such a state can account either for a high-spin Fe^{2+} ion or for the ground state arising from the intramolecular antiferromagentic coupling between the Fe^{3+} ($S = 5/2$) and Mo^{V} ($S = 1/2$) ions. The data indicate (vide infra) that either case can be treated in the framework of crystal field theory for a ^5D ion.

3.1. MAGNETIC SUSCEPTIBILITY

The effective magnetic moment of 4.9 Bohr magnetons is constant in the temperature range 100–300 K. This indicates that the $S = 2$ quintet spin state is the only populated state in this temperature range independent of its source of origin. The following spin Hamiltonian has been used to describe the zero field splitting of this state:

$$\mathcal{H}_s = D(S_z^2 - 3) + E(S_x^2 - S_y^2) + \mu_B H \cdot \underset{\sim}{g} \cdot S \,. \tag{1}$$

This Hamiltonian predicts the energy levels of the quintet state in terms of axial (D) and rhombic (E) parameters and the electronic g-tensor which reflects the influence of an external field H on these levels. The magnetic moment arising from each state i with energy E_i is

$$\mu_{ip} = -\frac{\partial E_i}{\partial H_p} = -\mu_B g_p \langle S_p \rangle \,,$$

where $p = x, y, z$ denote the principal axes of the D-tensor. The macroscopic magnetization of the system is described as the thermal average of the magnetic moments μ_{ip} [3]:

$$M_p = N_0 \frac{\sum\limits_{i=1}^{5} \mu_{ip}\, e^{-E_i/k_B T}}{\sum\limits_{i} e^{-E_i/k_B T}} \,,$$

where k_B is the Boltzmann constant and N_0 is the Avogadro number. For a polycrystalline sample, the magnetic susceptibility is the average of the corresponding values over the directions of the applied magnetic field in the D system of each crystallite:

$$\chi = \frac{M}{H} = \frac{1}{4\pi} \int\limits_{\theta=0}^{\pi} \int\limits_{\varphi=0}^{2\pi} [\chi_{xx} \cos^2\varphi \sin^2\theta + \chi_{yy} \sin^2\theta \sin^2\varphi + \chi_{zz} \cos^2\theta] \sin\theta \, d\theta \, d\varphi \,, \tag{2}$$

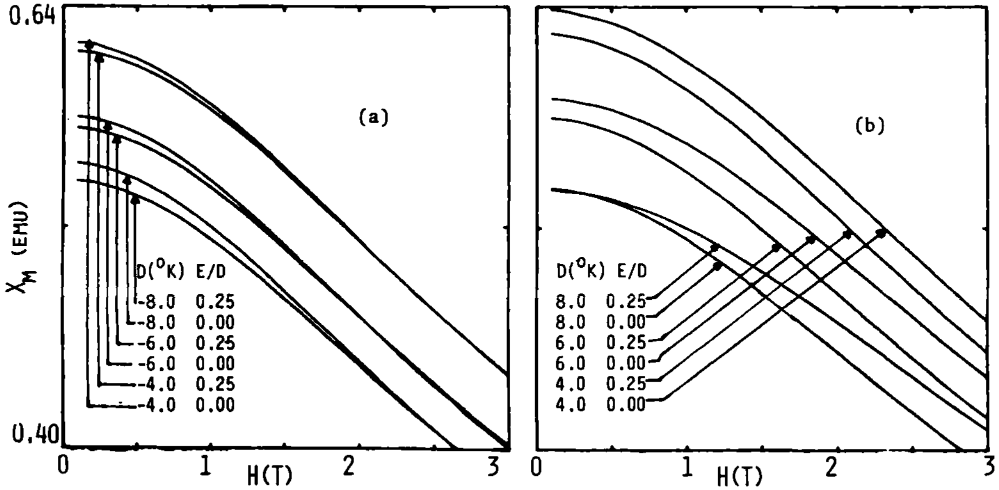

Fig. 1. Computations of the field dependence of the magnetic susceptibility for various combinations of D and E at 4.2 K for negative (a) and positive (b) D values ($g = 2$).

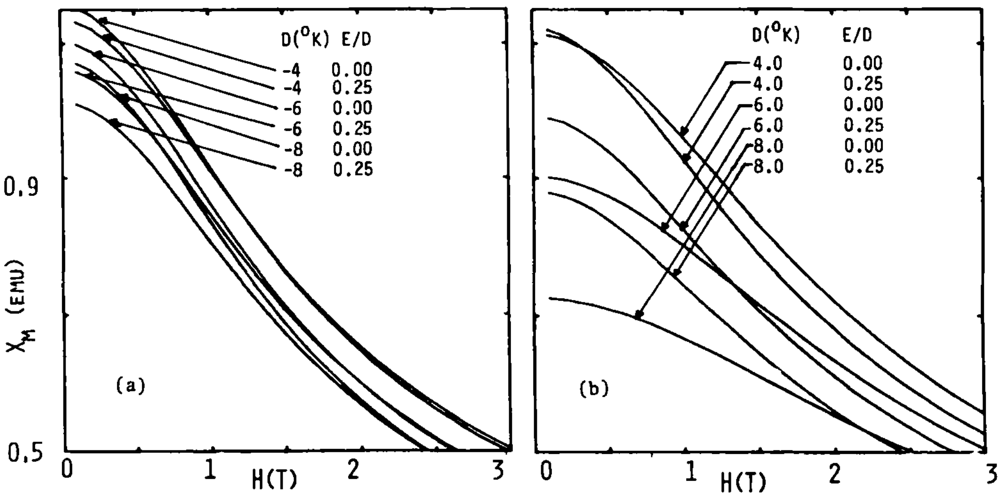

Fig. 2. Computations of the field dependence of the magnetic susceptibility for various combinations of D and E at 2 K for negative (a) and positive (b) D values.

where $\chi_{\ell\ell}$ is the tensor of the magnetic susceptibility. For a linear field dependence of magnetization, eq. (2) is reduced to:

$$\chi = \frac{1}{3}(\chi_{xx} + \chi_{yy} + \chi_{zz}), \tag{2a}$$

which is applicable at temperatures where the thermal energy $k_B T$ is larger than D and the magnetic energy $\mu_B H$.

As it turns out from the above description, five independent parameters (D, E, g_x, g_y, g_z) are required for the calculation of the magnetic susceptibility. Determination of these parameters by adjusting them to experimental data is a complicated problem which requires a well-defined methodology in order to obtain reliable results. Particularly difficult for powder samples is the determination of the sign of the axial parameter D and the value of the rhombic parameter E. In order to get some guidance for the influence of these parameters, we have computed the field dependence of the magnetic susceptibility at various temperatures (isotherms) on various combinations of the parameters. The main result of the search is that qualitative differentiation is achieved for the field dependence at temperatures comparable to the zero field splitting values D (4–10 K are typical D values for $S = 2$ ions in tetrahedral coordination). Figures 1 and 2 show the results of these computations for the temperatures 4.2 and 2 K and an average value g equal to 2. The following main conclusions can be drawn by comparing these two figures:

(1) The differences in the field dependence for values of D of opposite sign become most pronounced as D increases and the temperature decreases. (Compare, for example, the curves for $D = \pm$ 8 K at 2 K). For $D \lesssim 4$ K, lower temperatures than 2 K are required in order to determine the sign of D.

(2) The influence of the asymmetry parameter is more pronounced at low fields and at 2 K than at 4 K. Also the effect of varying E/D is stronger for $D > 0$ than at $D < 0$. (Compare, for example, curves for $E/D = 0$ and 0.25 in fig, 2(a) and 2(b).)

All the above considerations are direct consequences of the dependence of the spin state populations on the sign of D and the value of E/D in this temperature and magnetic field range [4].

Approximate values of the parameters D and g can be estimated initially by the following procedure: A value of the former can be evaluated from the temperature at which the effective magnetic moment approaches a constant value. All the spin states are populated at this temperature and for an $S = 2$ ion, the relation $4|D| \lesssim k_B T$ holds. For higher temperatures ($k_B T > 4D$), the Curie law holds for the temperature variation of the magnetic susceptibility and the average value of g can be determined from the relation [4]:

$$\chi_M = \frac{3}{4}\frac{\overline{g}^2}{T}, \tag{3}$$

where

$$\overline{g}^2 = \frac{1}{3}(g_x^2 + g_y^2 + g_x^2).$$

3.2. MÖSSBAUER DATA

The Mössbauer data have been analyzed by augmenting the electronic spin Hamiltonian (1) with the nuclear spin Hamiltonian:

$$\mathcal{H}_\mathrm{n} = \langle \boldsymbol{S}\rangle \cdot \underset{\sim}{A}(x'', y'', z'')\cdot \boldsymbol{I} + \mathcal{H}_\mathrm{q} - g_\mathrm{n}\,\mu_\mathrm{n}\,\boldsymbol{H}\cdot\boldsymbol{I}, \tag{4}$$

where

$$\mathcal{H}_\mathrm{q} = \frac{e^2 Q V_{z'z'}}{12}\,[3I_{z'}^2 - \tfrac{15}{4} + \eta(I_{x'}^2 - I_{y'}^2)]. \tag{5}$$

The symbols in eqs. (4) and (5) have their conventional definition and the various vectors and the reference frame systems for the respective diagonal tensors are denoted by (x, y, z) for the D tensor, (x', y', z') for the electric field gradient tensor (EFG) and (x'', y'', z'') for the hyperfine tensor A.

The above formalism is applicable for spectra in the limit of fast or slow spin relaxation (static case). For intermediate spin relaxation rates, we used the stochastic model by Clauser and Blume [5]. In this model, the line shape for Mössbauer absorption is calculated by:

$$I(\omega) = \mathrm{Re}\,F(p), \tag{6}$$

where

$$F(p) = \sum_{\text{all indices}} p_\nu \langle \nu n|A^+|\mu m\rangle\langle \mu m\,\nu n|\,U(p)|\mu' m'\nu' n'\rangle\langle \mu' m'|A|\nu' n'\rangle. \tag{7}$$

In this relation, ν, μ, ν', μ' and n, m, n', m' are indices labeling the electronic and nuclear states, respectively, p_ν is the occupation probability for the state ν, and A is an electromagnetic transition operator. The essential physics of the system is contained in the operator $U(p)$ given by:

$$U(p) = [P1 - \mathrm{i}\mathcal{H}_0^x - R]^{-1}\,, \tag{8}$$

where $p = \frac{1}{2}\Gamma - \mathrm{i}\omega$ and $\mathcal{H}_0^x$ is the Liouville operator corresponding to the total static Hamiltonian:

$$\mathcal{H}_0 = \mathcal{H}_\mathrm{s} + \mathcal{H}_\mathrm{n}\,.$$

The operator R carries the information on relaxation processes. In our calculation, we have used a simple model in which transitions between electronic states are induced by a fluctuating magnetic field H through the Hamiltonian:

$$\mathcal{H}_\mathrm{R} = g_\parallel \mu_\mathrm{B} S_z \bar{H}_z + g_\perp \mu_\mathrm{B}(S_x \bar{H}_x + S_y \bar{H}_y)\,. \tag{9}$$

Electronic transition probabilities are then calculated by the relations

$$W_{\mu\nu} = L\,p(\nu)|\langle\mu|\mathcal{H}_\mathrm{R}|\nu\rangle|^2\,, \tag{10}$$

where L is a rate constant for the fluctuating magnetic field and $p(\nu)$ is the occupation probability for the electronic state ν. Evaluation of (10) leads to parametrization of the transition probabilities with two phenomenological constants C_1 and C_2 given by:

$$C_1 = L\mu_\mathrm{B}^2 g_z^2 \bar{H}_z^2$$

$$C_2 = L\mu_\mathrm{B}^2 g_\perp^2 \bar{H}_\perp^2\,, \tag{11}$$

where $\bar{H}_z$ and $\bar{H}_\perp$ are time averaged components of the magnetic field.The constants C_1 and C_2 are then used as variable parameters in simulating the experimental spectra.

In a general case, the following parameters must be determined from the Mössbauer spectra: $D, E, A_x, A_y, A_z, \eta, g_x, g_y, g_z, C_1, C_2$, the Euler angles α, β, γ between the EFG tensor and the D tensor. The following assumptions, which are satisfactory approximations for the systems under study [4], were made in order to minimize the number of adjustable parameters:

(1) The A and D tensors are diagonal in the same reference frame.
(2) The Euler angle γ is equal to the angle α. This is a good assumption for small angles β (as it is justified by the final results of the complexes under study).
(3) The g-values were taken equal to those determined by the magnetic susceptibility data since the Mössbauer spectra are not sensitive to small deviations from the free electron g-value.

4. Results and discussion

4.1. MAGNETIC SUSCEPTIBILITY

Figure 3 shows the magnetic field dependence at temperatures 4.2 and 2.1 K and fig. 4 the temperature variation of the magnetization and the magnetic susceptibility for complex *A*. These variations are similar for all the studied complexes. The solid lines represent least-squares fit of the Hamiltonian (1) to the experimental data by applying the methodology briefly described in the following:

(1) A rough estimate of the value D is evaluated from the relation $k_B T \cong 4D$, where T is the temperature where magnetization reaches saturation, e.g. all the spin states of the quintet are populated. This value is in the range of 5 . . . 8 K for the four studied complexes. The average value of g can be determined from the high temperature magnetization data ($k_B T > 4D$) where relation (3) holds.

(2) The sign of D is determined from the magnetic field dependence of the magnetization at 4.2 and 2.1 K. By comparing the data of fig. 3, we note that the magnetic susceptibility value at $H = 2$ T is half the value it reaches at low fields ($H \sim 0.01$ T). Such behaviour corresponds to $D < 0$ according to the results of the computations presented in the previous section.

(3) The determination of D and the g_z components is done by fitting the 4.2 K data. Since D is negative, we assume that $g_\perp = g_x = g_y = \frac{1}{2}(3\bar{g}^2 - g_z^2)^{1/2}$. The g_z parameter space can be limited if we take values in the range $\bar{g} \ldots \bar{g} + 4D/\lambda$ according to second-order perturbation relations [6]. The spin-orbit coupling constant λ is set equal to 80 cm^{-1} in order to account for the covalency of the studied complexes [2]. An $E/D = 0.15$ value is estimated by comparing the data of fig. 3 with the calculations of fig. 1. By following this procedure, an accuracy of ± 1 K can be achieved for the D value and of ± 0.02 for the g components.

(4) The determination of the E/D value is done by fitting the data at 2.1 K using the values of $g_\perp$, g_z and D determined in the previous step.

At a final step, all these parameters are used as free parameters in a limited space fit of all the experimental data for further refinement and verification of their values. The results of this fit are shown in table 1. The negative sign of D indicates that the complexes have an easy axis of magnetization. The D values are within the range of 5 . . . 10 K, which is typical for an Fe^{2+} ion in tetrahedral coordination. This result suggests that a formal valence description of Fe(II)-Mo(VI) is appropriate for the binuclear metal core. An alternative formulation can also be proposed with an Fe(III) ($S = 5/2$) ion antiferromagnetically coupled to Mo(V) ($S = 1/2$) to give a resultant spin state of $S = 2$ for the cluster. In this case, the value of D entering in the spin Hamiltonian (1) for the resultant spin can be interpreted as a linear combination of the values for the two ions [7]. Since the values of D for Fe(III) in tetrahedral coordination with sulfur are of the order of $\lesssim 3$ K, it appears unlikely that a resultant

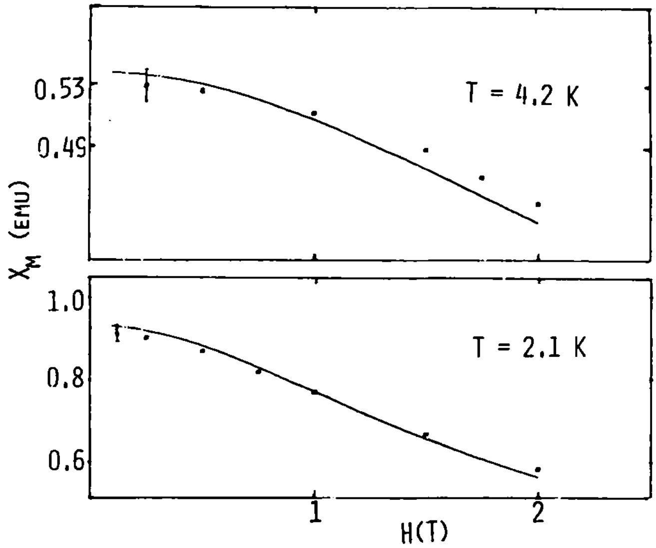

Fig. 3. Field dependence of the magnetic susceptibility of the $[(C_6H_5)_4P]_2$ $[(C_2H_5S)_2FeS_2MoS_2]$ complex at 4.2 K (top) and 2 K (bottom).

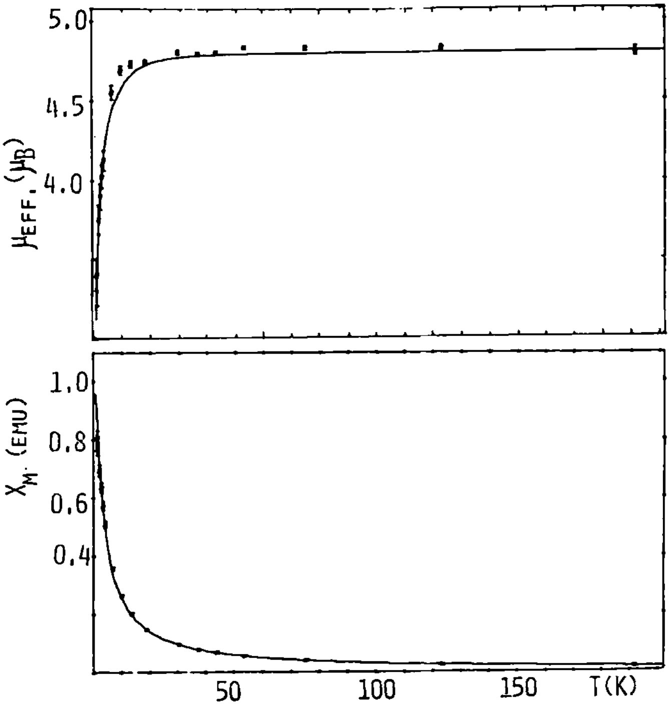

Fig. 4. Temperature variation of the magnetization (top) and magnetic susceptibility (bottom) of the $[(C_6H_5)_4P]_2$ $[(C_2H_5S)_2MoS_2]$ complex in an applied field of 1 T.

Table 1

Parameters of the spin Hamiltonian (1) determined from the magnetic susceptibility data

Complex	D (K)	E (K)	g	$g_{x,y}$	g_z
A	– 7.0(1.0)	2.2(5)	1.96(2)	1.95(2)	1.98(2)
A*	– 7.5(1.0)	2.3(5)	1.99(2)	1.98(2)	2.01(2)
B	– 6.0(1.0)	1.0(5)	1.98(2)	1.96(2)	2.02(2)
B*	– 9.0(1.0)	0.5(5)	2.01(2)	1.98(2)	2.07(2)

value of the magnitude found for the present complexes could be obtained. We conclude, therefore, that the most plausible valence description is Fe^{II}-Mo^{VI}. This conclusion is strongly supported by the hyperfine structure parameters obtained from the Mössbauer data (vide infra).

A small but systematic increase appears in the value of D in going from the Mo to the W homologue. Such a change can be correlated with the corresponding increase of the isomer shift in these complexes [2] and it could be attributed to different covalency between the two homologues.

The g-value appears slightly smaller than the free electron value g_e for all complexes except B*. This may be attributed to some diamagnetic impurity (~ 2%) in the samples. A systematic increase of this value in going from A to B*, however, is consistent with an increased ionicity, as witnessed by the corresponding increase of the isomer shift [2].

4.2. MÖSSBAUER DATA

Figures 5–7 show Mössbauer spectra of the studied complexes for selected combinations of temperature and applied magnetic field. The spectra were fitted with the spin Hamiltonians and relaxation formalism described in the previous section. A stepwise procedure, partly described in the literature [8], was followed in order to extract a physically meaningful set of parameters.

There are some qualitative features of the spectra, common for all complexes, which give a general idea regarding the behaviour of the electronic spin system in the presence of an external magnetic field. We notice first that the magnetic splitting at low temperatures saturates for relatively weak applied magnetic fields ($H \sim 0.9$ T). This implies that the electronic spin relaxation rate is slow at 4.2 K. Complex A is an exception, with relaxation rates being in the intermediate relaxation regime for these fields. The second point is that for intermediate applied fields ($0.9 < H < 3$ T), the spectra consist of reasonably sharp lines, despite the fact that the applied field has a

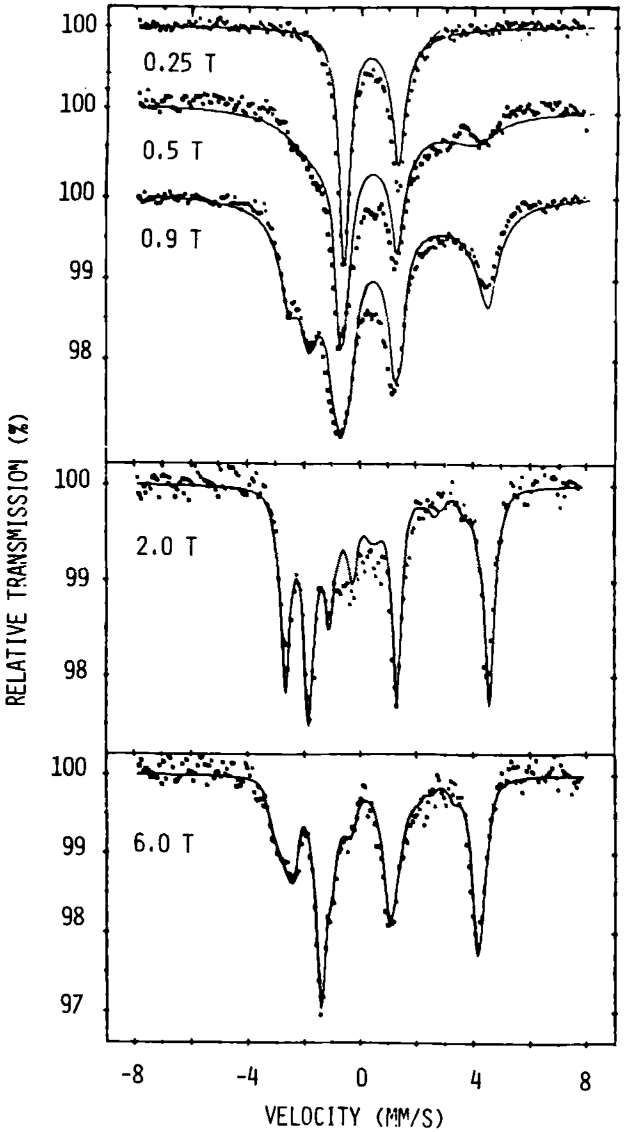

Fig. 5. Selected Mössbauer spectra of the $[(C_6H_5)_4P]_2$ $[(C_2H_5S)_2FeS_2MoS_2]$ complex at 4.2 K and various applied fields. The solid lines in the upper three spectra are simulations with the relaxation model discussed in the text, and those in the lower two spectra are the best fits in the slow relaxation limit.

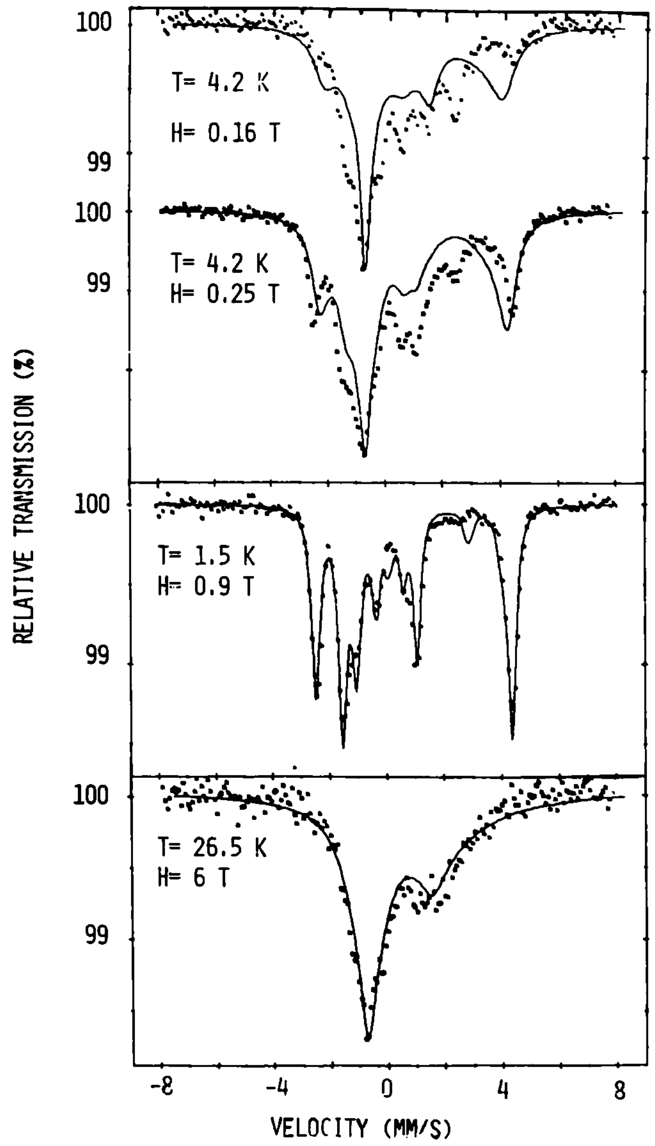

Fig. 6. Representative Mössbauer spectra of the $[(C_6H_5)_4P]_2$ $[(C_2H_5S)_2FeS_2WS_2]$ at various combinations of temperature and applied field. The solid lines are simulations with intermediate spin relaxation rates except for the spectrum at $T = 1.5$ K, $H = 0.9$ T, which represents the slow relaxation limit.

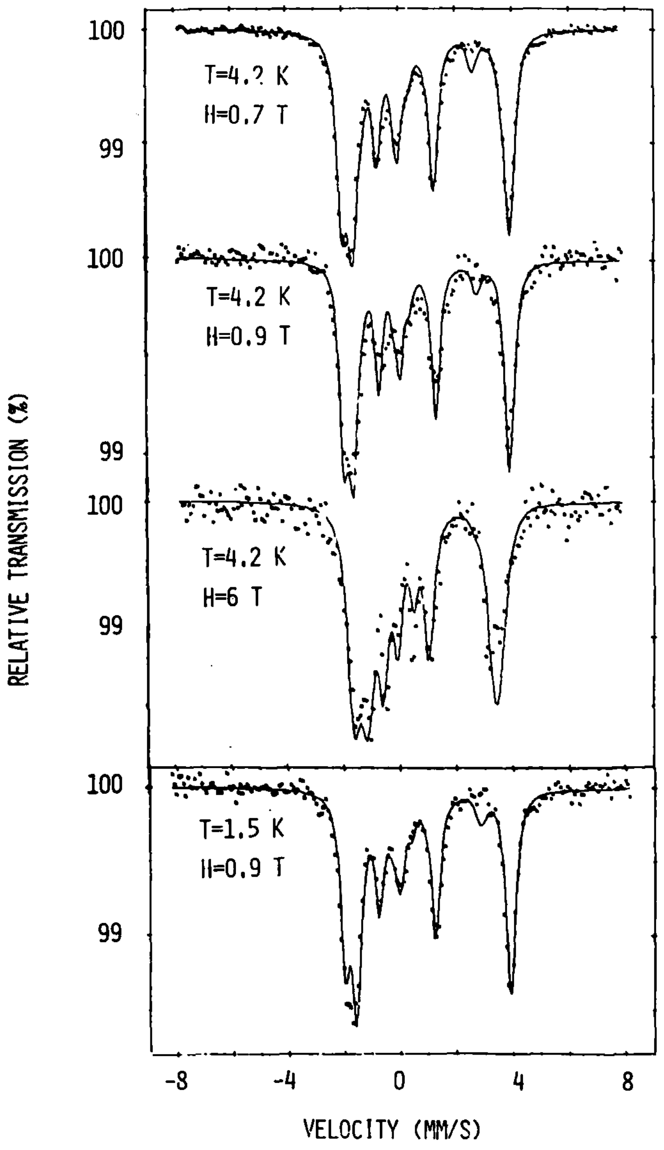

Fig. 7. Representative Mössbauer spectra of the $[(C_6H_5)_4P]_2\,[(S_5)FeS_2WS_2]$ at various combinations of temperature and applied field. The solid lines are the best fits to the experimental data in the slow relaxation limit.

different orientation with respect to the EFG axes of each molecule. This behaviour indicates a very anisotropic spin system. Finally, we notice that there is no significant change of the spectra at 1.5 and 4.2 K (fig. 7) in the presence of small magnetic fields. Therefore, only the lowest spin state is occupied in this temperature interval and, as the analysis shows [4], either $D \gtrsim 4$ K for $D < 0$ and $E/D < 0.25$ or $D \gtrsim 12$ K for $D > 0$ and $E/D > 0.25$. The first two points (saturation and axial anisotropy), however, favour the former case.

With the above considerations in mind, we proceed to the determination of the parameters of Hamiltonians (1) and (4) from the static (i.e. slow or fast relaxation limit) spectra. We select for each complex a spectrum with narrow lines which we can fit by assuming an internal magnetic field fixed in the molecular frame [9]. Thus, we can determine the sign of V_{zz}, the asymmetry parameter η and the direction of the internal field in the EFG system (angles θ and φ). For all cases, it was found that $\eta < 0.5$, $\theta \lesssim 10^\circ$ and $V_{zz} > 0$. The spectra were not sensitive to the value of angle φ. These results confirm that the studied complexes have an easy axis of magnetization and that the A and D tensors have the same principal frame. The value of A_z can also be determined from these data by using the saturation value of $S_z = 1.95$ [4]. As it turns out, from the high magnetic field spectra ($H > 2$ T) the sign of A_z is negative since the internal field is opposite to the applied magnetic field. Finally, the Euler angle β between the EFG and the A reference frames can be put equal to θ and $\alpha = \gamma = 0$. Having these parameters determined, we can attempt to fit the spectra to the Hamiltonians (1) and (4) with a limited number of varying parameters.

We first fit the spectra in small applied fields ($H \lesssim 2$ T). Computations of the quantum mechanical averages of $\langle S_z \rangle$ as a function of the applied field [4] show that in this range $\langle S_z \rangle$ is more sensitive to the value E/D than to D. Thus, in this step, only the E/D parameter was varied and the parameters D and $A_x = A_y = A_z$ were kept constant to the values determined by the magnetic susceptibility data and the nuclear spin Hamiltonian described in the previous paragraph. Best fits were achieved with repetitive simulations by slightly changing the fixed parameters in steps around their original values. In the final step, the high-field spectra ($H > 3$ T) were fitted with varying parameters D, A_x and A_y.

The results of the above calculations are listed in table 2. Inspection of this table shows that the parameter A_x is poorly determined. As detailed computations show [4], for D values of ~ 5 K, much higher fields than the available 6 T are required in order to more accurately determine the A_x parameter.

An inspection of table 2 shows some characteristic features which are common for the studied complexes. We notice first that $V_{zz} > 0$ and $\eta < 0.5$ in all cases. This, in combination with the negative D value and the fact that the z axes of the electronic spin Hamiltonian (1) and the EFG system are nearly parallel, indicates a $d_{x^2-y^2}$ main character for the electronic ground state [10]. Molecular orbital calculations based on an iterative extended Hückel theory have been reported recently for the complexes

Table 2

Fine and hyperfine parameters determined from the analysis of the Mössbauer data

Complex	D (K)	E (K)	η	A_x (mm/s)	A_y (mm/s)	A_z (mm/s)	β_{deg}
A	− 6(1)	1.8(3)	0.1(2)	1.2 − 1.6	1.10(5)	0.78(1)	10(2)
A*	− 7(1)	1.1(2)	0.3(1)	1.2 − 1.6	0.80(5)	0.65(1)	9(2)
B	− 5(1)	0.8(2)	0.3(1)	1.2 − 1.6	1.00(5)	0.73(1)	6(2)
B*	− 8(1)	1.0(2)	0.5(1)	1.1 − 1.6	0.80(5)	0.60(1)	4(2)

studied here [11]. They indicate that the highest doubly occupied MO is a mixture of Fe AO'S $|3z^2 - r^2\rangle$ and $|x^2 - y^2\rangle$, in close agreement with the above result. Another common feature is that $A_z/\bar{A} \cong 0.5$ and $\bar{A} = 1.12$ mm/s. The former value is characteristic of a high-spin ferrous ion [12]. In the antiferromagnetic coupling model on the other hand, with the valence assignment Fe(III)-Mo(V), the average value of the hyperfine tensor for Fe(III) referred to the total spin is $\bar{A} = \frac{7}{6}\,\bar{\alpha}\,(\mathrm{Fe}^{3+})$ [13], where $\alpha(\mathrm{Fe}^{3+}) = -22$ MHz from studies of oxidized rubredoxin [14]. This would give $\bar{A} = 1.26$ mm/s, which is larger than the value determined for the studied complexes. This, together with the characteristic anisotropy of the A tensor, favours the valence scheme of $\mathrm{Fe^{II}}$-$\mathrm{Mo^{VI}}$.

Intermediate relaxation effects are apparent in the spectra of the studied complexes at low fields ($H \lesssim 0.9$ T). Typical examples are the spectra of complex A at 4.2 K and $H = 0.25, 0.5, 0.9$ T (fig. 5) and of complex A* at 4.2 K and $H = 0.16$, 0.25 T (fig. 6). Table 3 shows the results of the simulations performed for spectra of

Table 3

Spin relaxation parameters derived from simulation of Mössbauer spectra in the intermediate regime

Complex	T (K)	H (T)	C_1 (cm/s)	C_2 (cm/s)
A	1.4	0.9	0.09(2)	
	4.2	0.2	0.15(2)	
	4.2	0.5	0.15(2)	
	4.2	0.9	0.13(3)	
	25.6	6.0	2.0 (3)	2.5(3)
A*	4.2	1.6	0.05(2)	
	4.2	2.5	0.05(2)	
	25.6	6.0	1.5 (3)	1.5(3)

the complexes A, A^* with spin relaxation in the intermediate regime. For these simulations, we have used the formalism described in the previous section with zero field splitting and hyperfine parameters those of table 2, and by varying the phenomenological parameters C_1 and C_2 [eq. (7)]. It was not possible to obtain reliable values for these parameters for complexes B and B^* due to the complications present in these spectra from a possible spontaneous ordering at ~ 10 K and the existence of a second (minority) iron site in B [2].

The model employed for simulation of spectra with intermediate spin relaxation gives satisfactory results only for the spectra taken in applied fields $H \gtrsim 0.5$ T. It seems that strongly anisotropic mechanisms are present for the low field cases. Although some trends are apparent (table 3) for the temperature variation of the parameters C_1 and C_2, these data are not sufficient to draw any conclusions on the prevailing relaxation mechanism (spin-spin or spin-lattice) in the present systems. Finally, the spin relaxation is systematically faster for the Mo than the W homologues, a fact which may be related to the observed different charge delocalization between these complexes.

5. Conclusions

The following are the main conclusions which can be drawn from the present study:

(a) By following a certain methodology, it is possible to derive from low-temperature magnetic susceptibility measurements the value and sign of the parameters D and E/D.

(b) These values are confirmed within experimental error by an independent analysis of Mössbauer spectra in the presence of external magnetic fields.

(c) D is negative for all complexes and nearly parallel to the V_{zz} axis.

(d) Both fine and hyperfine parameters point to a valence scheme of Fe^{II}-Mo^{VI} with a varying degree of charge delocalization.

(e) Intermediate spin relaxation is present under certain conditions of temperature and applied field, while anisotropic mechanisms may be necessary to explain the more complicated cases.

References

[1] D. Coucouvanis, Acc. Chem. Res. 14(1981)201.

[2] D. Coucouvanis, P. Stremple, E.D. Simhon, D. Swenson, N.C. Baenziger, M. Draganjac, L.T. Chan, A. Simopoulos, V. Papaefthymiou, A. Kostikas and V. Petrouleas, Inorg. Chem. 22(1983)293.

[3] C.J. Ballhausen, *Introduction to Ligand Field Theory* (McGraw–Hill, New York, 1962).

[4] V. Papaefthymiou, Ph.D. Thesis, University of Ioannina (1984).

[5] M.J. Clauser and M. Blume, Phys. Rev. B3(1971)583.
[6] R. Zimmerman, H. Spiering and G. Ritter, Chem. Phys. 4(1974)133.
[7] J. Owen and E.A. Harris, *Electron Paramagnetic Resonance,* ed. S. Geschwind (Plenum Press, New York, 1972) Ch. 6.
[8] R. Zimmerman, B.H. Huynh and E. Münck, J. Chem. Phys. 69(1978)5463, and references therein.
[9] W. Kundig, Nucl. Instr. Meth. 48(1967)219.
[10] V. Petrouleas, A. Simopoulos, A. Kostikas and D. Coucouvanis, J. de Phys. 37(1976)C6-159
[11] A.X. Trautwein, E. Bill, R. Bläs, S. Lauer, H. Winkler and A. Kostikas, J. Chem. Phys. 82 (1985)3584.
[12] T.A. Kent, K. Spartalian and G. Lang, J. Chem. Phys. 71(1979)4899.
[13] S. Griffith, Structure and Bonding 10(1972)87.
[14] C. Schulz and P.G. Debrunner, J. de Phys. 37(1976)C6-153.